

# Large and Complex Chromatic Dispersion Profile in Epsilon-Near-Zero Aluminum-Doped Zinc Oxide

Jiaye Wu<sup>1</sup>, Ze Tao Xie<sup>1</sup>, Yanhua Sha<sup>1</sup>, H. Y. Fu<sup>2</sup>, Qian Li<sup>1,\*</sup>

<sup>1</sup> School of Electronic and Computer Engineering, Peking University, Shenzhen 518055, China

<sup>2</sup> Tsinghua-Berkeley Shenzhen Institute (TBSI), Tsinghua University, Shenzhen 518055, China

\* [liqian@pku.sz.edu.cn](mailto:liqian@pku.sz.edu.cn)

**Abstract:** We demonstrate the large and complex chromatic dispersion profile in epsilon-near-zero aluminum-doped zinc oxide. Results show very large and rapidly varying dispersion profile, and reveal its unsuitability for dispersion compensation devices. © 2020 The Author(s)

**OCIS codes:** 310.7005, 260.2030, 230.2035, 130.2035.

## 1. Introduction

As a novel platform for photonics and integrated optics, epsilon-near-zero (ENZ) materials have given rise to heated discussions in multiple subdisciplines of physics. Current theoretical investigations on ENZ materials reveal extraordinary optical properties such as electric field enhancement [1], large Kerr nonlinear effect [2], and femtosecond pulse dynamics in subwavelength setup [3]. Experimental studies on ENZ transparent conducting oxides (TCOs) have also explored large optical nonlinearity [4] and high harmonic generation [5,6] within the ENZ region where the real part of the complex permittivity gradually crosses zero. In this work, we theoretically demonstrate that, as a kind of TCOs, aluminum-doped zinc oxide (AZO) has complex and large  $N$ -th order chromatic dispersions in its ENZ regime. Rapidly varying and nonzero first to fourth-order dispersions exist near the ENZ point and their values are unprecedentedly large. For example, the second-order dispersion for AZO can reach  $0.32 \text{ fs}^2/\text{nm}$ , which is significantly larger than the highly dispersive indium phosphide (InP) waveguide ( $\sim 0.0296 \text{ fs}^2/\text{nm}$ ). It is also found that although the dispersion is large, utilizing this property for dispersion management is nearly impossible due to mismatches between each order of dispersions.

## 2. Theoretical Models

The Drude model is known to illustrate the real and imaginary parts of the complex permittivity of AZO accurately and agrees with experimental results:

$$\varepsilon_R = \varepsilon_r + i\varepsilon_i = \varepsilon_b - \frac{\omega_p^2}{(\omega^2 + \gamma^2)} + i \frac{\omega_p^2 \gamma}{(\omega^2 + \gamma^2) \omega}, \quad (1)$$

where  $\varepsilon_r$  is the real part,  $\varepsilon_i$  is the imaginary part associated with the intrinsic loss of AZO.  $\varepsilon_b = 3.85$  is the background permittivity,  $\omega$  is the angular frequency of light,  $\omega_p = 2.38 \times 10^{15} \text{ rad/s}$  is the plasma frequency determined by the free carrier concentration, and  $\gamma = 6.80 \times 10^{13} \text{ rad/s}$  is the damping rate (Drude relaxation rate) which signifies the scattering rate of electrons [7]. The ENZ wavelength (ENZ point)  $\lambda_{\text{ENZ}}$  where  $\varepsilon_r$  vanishes to zero is  $1550 \text{ nm}$ . The obtained complex permittivity versus wavelength is plotted in Fig. 1(a). By using the generalized Maxwell's relation  $\varepsilon_r = n^2 - k^2$ ,  $\varepsilon_i = 2nk$ , the complex permittivity can be converted to the complex refractive index  $n + ik$ , where the extinction coefficient  $k$  also denotes the loss term. The variation of  $n$  and  $k$  is shown in Fig. 1(b). It can be deduced that within the ENZ region, the refractive index is smaller than one but always greater than zero due to the nonzero  $\varepsilon_i$ , even at wavelengths longer than ENZ point with negative  $\varepsilon_r$ . Also, the fast-declining  $\varepsilon_r$  results in a sharp turning in the  $n$  curve, leading to dispersion profiles that feature potentially large values and rapid variations in multiple orders. Due to near-zero permittivity and near-zero refractive index, these characteristics are exclusive to ENZ materials.

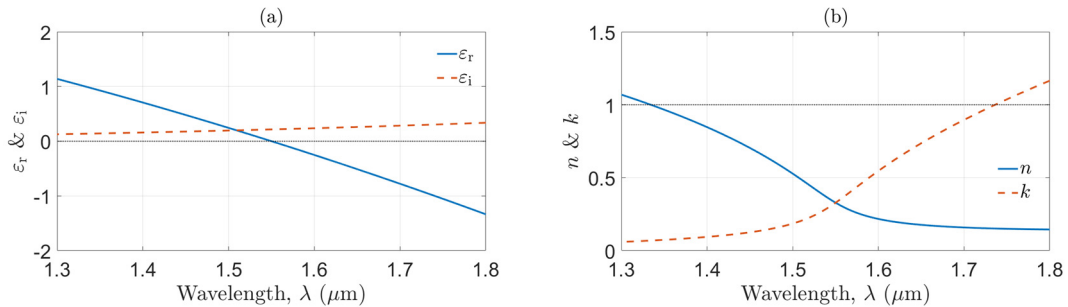


Fig. 1. The variation of (a) complex permittivity and (b) complex refractive index of ENZ AZO near  $\lambda_{\text{ENZ}} = 1550 \text{ nm}$ . (a) The solid line represents  $\varepsilon_r$ , and the dashed line represents  $\varepsilon_i$ . (b) The solid line represents  $n$  and the dashed line represents  $k$ .

### 3. Complex Chromatic Dispersion Profile

By definition, the propagation coefficient (also known as the wavenumber) is  $\beta = n\omega/c$ , and each order of dispersion is obtained from its Taylor expansion coefficient that  $\beta_N \equiv d^N\beta/d\omega^N$ . Using symbolic computation,  $\beta$  can be expressed analytically using parameters from the Drude model as  $\beta(\omega, \varepsilon_b, \omega_p, \gamma)$ :

$$\beta(\omega, \varepsilon_b, \omega_p, \gamma) = \frac{n\omega}{c} = \frac{\sqrt{2}\omega}{2c} \sqrt{\varepsilon_b + \sqrt{\left(-\frac{\omega_p^2}{\gamma^2 + \omega^2} + \varepsilon_b\right)^2 + \frac{\gamma^2 \omega_p^4}{\omega^2 (\gamma^2 + \omega^2)^2}} - \frac{\omega_p^2}{(\gamma^2 + \omega^2)}}. \quad (2)$$

Therefore, by the same technique, each  $\beta_N$  can also be deduced analytically. By substituting three Drude parameters, the results of  $\beta_1$  to  $\beta_4$  are illustrated in Fig. 2 as examples. In Fig. 2(b), the maximum normal second-order dispersion value is 0.32 fs<sup>2</sup>/nm, which is significantly larger than the highly dispersive InP waveguide ( $\sim 0.0296$  fs<sup>2</sup>/nm). The maximum absolute values for third- and fourth-order dispersions are, -16.25 fs<sup>3</sup>/nm at 1538 nm and -1235 fs<sup>4</sup>/nm at 1556 nm, respectively. It is worth noting that,  $\varepsilon_b$  and  $\gamma$  can vary within a range due to many factors in fabrication processes and defects in different samples, which will lead to slightly different curves and values, but their tendency would agree with Figs. 2(a)-2(d). In theory, all ENZ TCOs that resemble AZO would have infinite orders of nonzero dispersions near ENZ point, and allows complicated dynamic patterns to emerge when nonlinearity is taken in to account, for example, in Ref. [3]. Although the aforementioned dispersion values are large, utilizing this property to design a compact dispersion compensation device is nearly impossible. From Figs. 2(a)-2(d), the zero-dispersion points for each order spread across 1540-1560 nm, and the maximum positive and negative dispersion values are located in different spectral locations across different orders, making it hard to align them and perform dispersion management in ENZ TCOs.

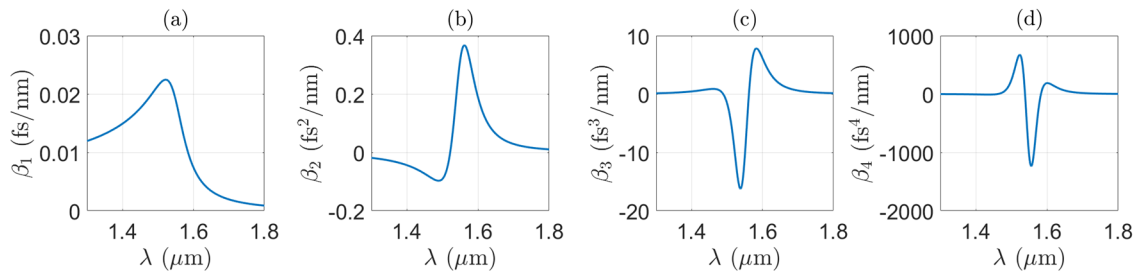


Fig. 2. The variation of (a) first-, (b) second-, (c) third-, and (d) fourth-order dispersions of ENZ AZO near  $\lambda_{\text{ENZ}} = 1550$  nm.

### 4. Conclusion

We theoretically demonstrate that AZO exhibits large and complex  $N$ -th order chromatic dispersion profile in its ENZ regime near the telecom wavelength of 1550 nm. Unprecedentedly large and rapidly varying nonzero first to fourth-order dispersions exist near the ENZ point. At the same wavelength, the second-order dispersion for AZO can reach 0.32 fs<sup>2</sup>/nm, which is significantly larger than the highly dispersive InP waveguide. However, this high dispersion profile is found to be not suitable for designing compact dispersion compensation devices, due to wavelength mismatch between the maximum dispersion in each order.

### Acknowledgments

This work is supported by the National Natural Science Foundation of China (61675008), Shenzhen Science and Technology Innovation Commission (GJHZ2018411185015272, JCYJ20180507183815699), and Youth Science and Technology Innovation Talent of Guangdong Province (2019TQ05X227).

### References

- [1] S. Campione, D. de Ceglia, M. A. Vincenti, M. Scalora, and F. Capolino, "Electric field enhancement in  $\varepsilon$ -near-zero slabs under TM-polarized oblique incidence," *Phys. Rev. B* **87**, 035120 (2013).
- [2] A. Ciattoni, C. Rizza, A. Marini, A. Di Falco, D. Faccio, and M. Scalora, "Enhanced nonlinear effects in pulse propagation through epsilon-near-zero media," *Laser Photon. Rev.* **10**, 517–525 (2016).
- [3] J. Wu, B. A. Malomed, H. Y. Fu, and Q. Li, "Self-interaction of ultrashort pulses in an epsilon-near-zero nonlinear material at the telecom wavelength," *Opt. Express* **27**, 37298–37306 (2019).
- [4] M. Z. Alam, I. De Leon, and R. W. Boyd, "Large optical nonlinearity of indium tin oxide in its epsilon-near-zero region," *Science* **352**, 795–797 (2016).
- [5] A. Capretti, Y. Wang, N. Engheta, and L. Dal Negro, "Comparative Study of Second-Harmonic Generation from Epsilon-Near-Zero Indium Tin Oxide and Titanium Nitride Nanolayers Excited in the Near-Infrared Spectral Range," *ACS Photonics* **2**, 1584–1591 (2015).
- [6] L. Rodríguez-Suné, M. Scalora, A. S. Johnson, C. Cojocaru, N. Akozbek, Z. J. Coppens, D. Perez-Salinas, S. Wall, and J. Trull, "Study of second and third harmonic generation from an indium tin oxide nanolayer: Influence of nonlocal effects and hot electrons," *APL Photonics* **5**, 010801 (2020).
- [7] G. V. Naik, V. M. Shalae, and A. Boltasseva, "Alternative Plasmonic Materials: Beyond Gold and Silver," *Adv. Mater.* **25**, 3264–3294 (2013).